

Dynamics of a droplet under the influence of an alternating electric field

Jay Chaudhari[†], Manoj Kumar Tripathi[†], Suman Chakraborty^{††} and Kirti Chandra Sahu^{*}

[†]Indian Institute of Science Education and Research Bhopal 462 066,

Madhya Pradesh, India

^{††}Department of Mechanical Engineering,
Indian Institute of Technology Kharagpur,
Kolkata 721302, India

Department of Chemical Engineering,
Indian Institute of Technology Hyderabad,
Kandi, Sangareddy 502 285, Telangana, India

(Dated: June 2, 2022)

We investigate the electrohydrodynamics of an initially spherical droplet in a leaky dielectric medium under the influence of an external AC electric field by conducting axisymmetric numerical simulations using a charge-conservative volume-of-fluid based finite volume flow solver. The droplet and the surrounding medium are assumed to have the same density and the same viscosity. The experimental study of [29] reported that along the zero circulation line (i.e. when electrical conductivity ratio, K_r is equal to the permittivity ratio, S), the mean deformation of a droplet in an applied AC electric field, $E_{AC}(t)$ is equal to the steady state deformation in a DC field, E_{DC} equals to the root-mean-square of $E_{AC}(t)$. However, in two-dimensional simulations, it is observed that the droplet deformation behaviours are similar under both AC and the equivalent DC electric fields even for the values of (S, K_r) away from the zero circulation line. This motivates us to revisit this problem by performing axisymmetric simulations. The main findings of our study are (i) for $K_r \neq S$, the droplet deformation shows strikingly different behaviour in case of an AC and the equivalent DC fields, (ii) unlike the previous numerical studies, the results obtained from our axisymmetric simulations are consistent with the experimental investigation of [29], and (iii) the parametric study conducted for a wide range of parameters reveals that in case of an AC electric field, the droplet oscillates about a prolate shape; increasing the time period of the electric field (T_p) increases the amplitude of shape oscillations; however, the time period of the oscillations is always observed to be equal to $T_p/2$. Increasing S and K_r has a nonmonotonic effect on the degree of deformation of the droplet, which is minimum for $K_r = S$. In contrast, for the equivalent DC electric field, for $K_r < S$, the droplet deforms to a steady oblate shape after deforming to an early prolate shape, but for $K_r > S$, the droplet continues to deforms monotonically and obtains a steady prolate shape.

I. INTRODUCTION

The electrohydrodynamics (EHD) of a liquid droplet suspended in another medium has been a subject of research from several decades due to its relevance in industrial applications [2], microfluidics [11, 15, 19, 24], biological systems [31] and natural phenomena such as electrification of rain, raindrops bursting in thunderstorms and electrification of the atmosphere [16, 22, 33]. An extensive review of earlier work on EHD of a droplet can be found in [13].

The pioneering work of [29] provided a deformation-circulation map in the electrical conductivity ratio, $K_r (\equiv K_i^*/K_o^*)$ and the permittivity ratio, $S (\equiv \epsilon_i^*/\epsilon_o^*)$ plane, which has been used to study EHD of a droplet under the influence of alternating (AC) electric field (see e.g. [5]). Here, ϵ_i^* , K_i^* and ϵ_o^* , K_o^* are the dimensional electrical permittivity and conductivity of the droplet and surrounding fluid, respectively. This map (shown in Fig. 1) delineates three different regions classified in terms of droplet deformation and flow field. The regions are separated by the so-called the zero-circulation line ($S = K_r$) along which the mean velocity field is zero and zero-deformation curve ($K_r^2 + K_r + 1 - 3S = 0$). In region I, the droplet deforms to a prolate (oblate) shape if $2\pi/T_p > \omega_{cr}$ ($2\pi/T_p < \omega_{cr}$); for $2\pi/T_p = \omega_{cr}$ the droplet remains spherical, such that $\omega_{cr} = K_o^* \sqrt{3S - 1 - K_r - K_r^2}/\epsilon_o^* |S - 1|$ and T_p denotes the time period of the imposed AC electric field. In regions II and III, the droplet deforms to a prolate shape with a flow from poles to the equator and equator to the poles, respectively.

In EHD, based on the time scales associated with the decay of free charge density, ρ_e around a droplet of radius R ($t_e = \epsilon_o/K_o$; also known as the electric relaxation time) and the viscous time scale ($t_v = R^2/\nu$), the fluid can be classified as perfect and leaky dielectric media [20]; ν being the kinematic viscosity. In a leaky dielectric medium,

* ksahu@iith.ac.in

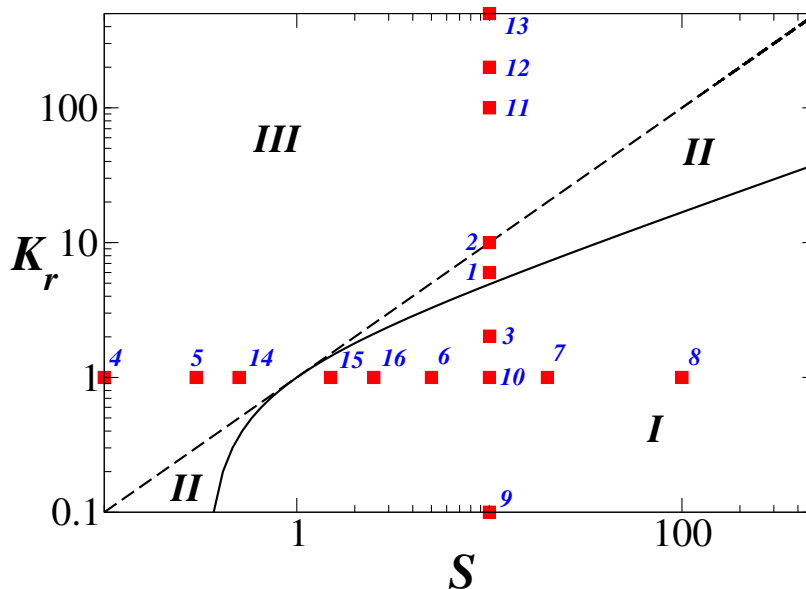


FIG. 1: The deformation-circulation map reported by [29] to study electrohydrodynamics of a droplet under an AC electric field. The dashed and solid lines correspond to $S = K_r$ (the zero-circulation line) and $K_r^2 + K_r + 1 - 3S = 0$ (the zero-deformation curve). The red filled square symbols represent the values of S and K_r considered in our simulations.

$t_e \ll t_v$, which implies that the charge accumulates at the interface almost instantaneously. In other words, in a leaky dielectric medium, the charge conservation in the bulk fluid reaches to a steady state much faster than the fluid motion. A medium with $t_e \gg t_v$ is termed as perfect dielectric, in which $\rho_e = 0$. The present study deals with a leaky dielectric medium.

The electrohydrodynamics of a droplet under the action of an applied direct current (DC) electric field have been investigated by several researchers in the past considering perfect [6, 7, 21] and leaky dielectric media [15, 28]. [25] proposed an electrohydrodynamics theory to study small deformation of a neutrally buoyant droplet in a leaky dielectric medium, which has been used by many authors to validate their numerical solvers. [28] demonstrated that their coupled-level-set-volume-of-fluid (CLSVOF) method based EHD flow solver predicts the theoretically obtained droplet deformation under an applied DC electric field in both perfect and leaky dielectric media. [6] investigated droplet deformation in an applied DC electric field using an axisymmetric front tracking/finite volume method and demonstrated that a droplet with net surface charge deforms into a prolate shape, and moves along the electric field. Later, [8] proposed a charge-conservative scheme to solve EHD of interfacial flows using volume of fluid (VoF) method for perfect and leaky dielectric media and validated their solver by comparing with the previous studies. They also suggested a correction to the expression of droplet deformation presented in [6] which appears due to the nondimensionalisation of the theoretical expression proposed by [25]. [23] developed a lattice Boltzmann method based EHD solver to study the droplet deformation in a leaky dielectric medium. [35] analytically studied the dynamics of a toroidal drop freely suspended in another fluid subjected to a uniform electric field. [4] investigated the deformation and dynamics of a liquid drop under the application of a DC electric field in a leaky dielectric medium. The rise dynamics of a bubble under the combined action of gravity and a uniform electric field applied in the vertical direction was studied by [32]. They showed that electric field elongates and accelerates the motion of the bubble in the vertical direction. In addition, several recent studies have been reported on EHD of droplets under DC field, employing asymptotic, numerical and experimental approaches ([1, 9, 10, 12, 17, 19]; references therein). These studies despite addressing some fundamental aspects of EHD of droplets, turn out to be inadequate in explaining the morpho-dynamic evolution of droplets under alternating electric fields.

As discussed above, although a large number of investigations have focused on droplet deformation in DC electric field, dynamics of a droplet under the action of AC electric field has received comparatively less attention [14, 27, 30]. Most relevant here is a recent study of [5], who investigated the EHD of a neutrally buoyant liquid droplet under the application of an AC electric field by conducting two-dimensional simulations in a perfectly dielectric medium. They found that the mean deformation of the droplet under the influence of an AC electric field can be represented by the steady-state deformation in an equivalent DC electric field in a root-mean-square sense in all the regions presented in Fig. 1. However, [29] reported that the mean deformation of a droplet in an AC electric field, $E_{AC}(t)$ is the same as the steady state deformation in a DC electric field, E_{DC} equals to the root-mean-square of $E_{AC}(t)$

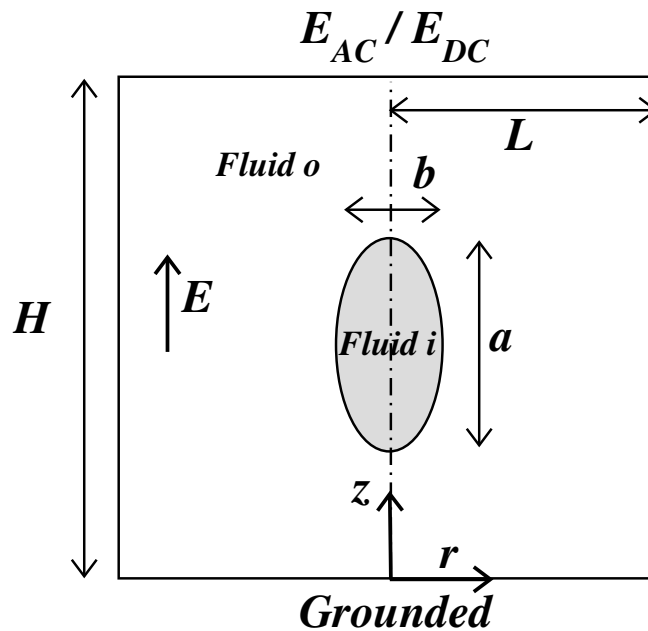


FIG. 2: Schematic diagram (not to scale) of a droplet (fluid ‘*i*’) in another immiscible fluid (fluid ‘*o*’) under an AC electric field (E_{AC}) or DC electric field (E_{DC}) applied in the axial direction.

only along the zero circulation line (i.e. along $S = K_r$ line in Fig. 1). This motivates us to revisit this problem by performing axisymmetric simulations in the present study. We found that axisymmetric simulations predict the behaviour observed by [29]. A parametric study is also conducted by varying the time period of the applied AC electric field, the permittivity and the electrical conductivity ratios. The droplet deformation and the flow field in case of an AC electric field are compared with those obtained in the equivalent DC electric field. For the parameters considered in the present study, the droplet becomes prolate (elongates in the direction of electric field) and oscillates about a mean value of the degree of deformation (defined below) in an AC electric field. However, for high permittivity and low electrical conductivity ratios, the droplet becomes oblate in case of a DC electric field. This behaviour is similar to that observed in the experiments of [29].

The paper is organized as follows. The problem is formulated in Section II, wherein the governing equations, numerical method and validation of the present solver are discussed in detail. The results are presented in Section III and concluding remarks are given in Section IV.

II. FORMULATION

The dynamics of an initially spherical droplet of radius R inside another immiscible fluid under the influence of an external electric field is investigated via axisymmetric numerical simulations. A schematic diagram of the configuration considered in the present study is shown in Fig. 2. The droplet (fluid ‘*i*’) and the surrounding liquid (fluid ‘*o*’) are assumed to be incompressible and Newtonian. In order to isolate the effect of electric field from other forces (such as gravity) on the droplet dynamics, the fluids are also assumed to have the same density, ρ^* and the same viscosity μ^* . An axisymmetric cylindrical coordinate system (r, z) is used to model the flow dynamics. The droplet deformation is investigated under the influence of an AC electric field, given by

$$E_{AC}(t) \equiv \frac{\psi_{AC}(t)}{H} = \frac{\psi_0}{H} \sin\left(\frac{2\pi t}{T_p}\right). \quad (1)$$

Here, t represents time; $E_{AC}(t)$, $\psi_{AC}(t)$ and ψ_0 are the dimensionless electric field, electric potential and its magnitude, respectively.

The electric field is applied at the top wall at $z = H$ by connecting to an AC power source and the bottom wall at $z = 0$ is grounded. The droplet deformation in the presence of the AC electric field is compared against that observed in an equivalent DC electric field (E_{DC}) with its magnitude equal to the root-mean-squared (rms) magnitude of the

AC electric field, such that

$$E_{DC} = \frac{\psi_{DC}}{H} = \lim_{t \rightarrow \infty} \sqrt{\frac{1}{2T_p} \int_{-T_p}^{T_p} \left(E_0 \sin \left(\frac{2\pi t}{T_p} \right) \right)^2 dt} = \frac{E_0}{\sqrt{2}}, \quad (2)$$

wherein $E_0 = (\psi_0/H)$ and ψ_{DC} is the electric potential of the equivalent DC field.

An axisymmetric computational domain of size $(H \times L) = (8R \times 8R)$ is considered in the present study. Initially, the centre of the droplet is kept at $(0, 4R)$. The following boundary conditions are used. No-slip and no-penetration conditions are imposed at the top and bottom boundaries at $z = H, 0$; free-slip boundary condition is applied at $r = L$, and symmetry boundary condition is imposed at $r = 0$.

Under the influence of electric field the initially spherical droplet deforms to an ellipsoid shape with a and b as the length and breadth of the droplet in the directions parallel and perpendicular to the applied electric field. Thus, the degree of deformation, D can be defined as $(a - b)/(a + b)$, such that $D > 0$ and $D < 0$ correspond to a prolate and an oblate shape, respectively; $D = 0$ represents a spherical droplet.

A. Governing equations

Under the influence of an electric field the droplet dynamics is governed by the continuity and the Navier-Stokes equations with an additional body force term associated with the electric field (\mathbf{f}_e). In the dimensionless form the governing equations are given by

$$\nabla \cdot \mathbf{u} = 0, \quad (3)$$

$$\rho \left(\frac{\partial \mathbf{u}}{\partial t} + \mathbf{u} \cdot \nabla \mathbf{u} \right) = -\nabla p + \frac{1}{Re} \nabla \cdot [\mu(\nabla \mathbf{u} + \nabla \mathbf{u}^T)] + \delta(\mathbf{r} - \mathbf{r}_f) \frac{\nabla \cdot \mathbf{n}}{We} \mathbf{n} + \mathbf{f}_e, \quad (4)$$

$$\nabla \cdot (\epsilon \nabla \psi) = -\chi \rho_e, \quad (5)$$

$$\mathbf{E} = -\nabla \psi. \quad (6)$$

$$\frac{\partial \rho_e}{\partial t} + \nabla \cdot (\rho_e \mathbf{u}) = \frac{1}{\chi O_c} \nabla \cdot (K \nabla \psi), \quad (7)$$

where, $\mathbf{u} = (u, w)$ denotes the velocity field; u and w represent the velocity components in the r and z directions, respectively; p is pressure field; $\delta(\mathbf{r} - \mathbf{r}_f)$ is a delta function which is zero everywhere except at the interface, i.e. at $\mathbf{r} = \mathbf{r}_f$; \mathbf{n} is the unit normal to the interface pointing towards fluid 'o'. The body force due to the applied electric field is given by: $\mathbf{f}_e = \nabla \cdot \mathcal{M} = \rho_e \mathbf{E} - \mathbf{E}^2 \nabla \epsilon / 2\chi$; \mathcal{M} being the Maxwell's stress tensor, ϵ represents the electric permittivity and ρ_e is the volumetric charge density.

In addition to Eqs. (3) - (7), we solve the following advection equation for the volume fraction, c of fluid 'i' in order to track the interface separating the droplet ($c = 1$) and outer fluid ($c = 0$):

$$\frac{\partial c}{\partial t} + \mathbf{u} \cdot \nabla c = 0. \quad (8)$$

The dimensionless permittivity and electrical conductivity are given by

$$\epsilon = (1 - c) + cS, \quad (9)$$

$$K = (1 - c) + cK_r. \quad (10)$$

The governing equations have been non-dimensionalised using the initial radius of the droplet, R as the length scale, $\sqrt{\gamma^*/\rho^*R}$ as the velocity scale (V_s) and $\sqrt{\gamma^*/R\epsilon_0^*}$ as the characteristic electric field strength (E_s) and the material properties of the surrounding medium as the corresponding characteristics scales. The interfacial surface tension is denoted by γ^* . The various dimensionless numbers appearing in Eqs. (3)-(10) are the Reynolds number ($Re(\equiv \rho^*V_sR/\mu^*)$), the electrical conductivity ratio ($K_r(\equiv K_i^*/K_o^*)$), the permittivity ratio ($S(\equiv \epsilon_i^*/\epsilon_o^*)$), and the dimensionless number associated with Ohmic charge conduction, O_c is $V_s\epsilon_o^*/K_o^*R$. In addition to these dimensionless numbers, there are two more dimensionless numbers, namely the Weber number ($We(\equiv \rho V_s^2 R/\gamma^*)$) and the electro-gravitational number ($\chi(\equiv \rho^*V_s^2/\epsilon_o^*E_s^2)$), which are equal to one due to the present choice of the scales.

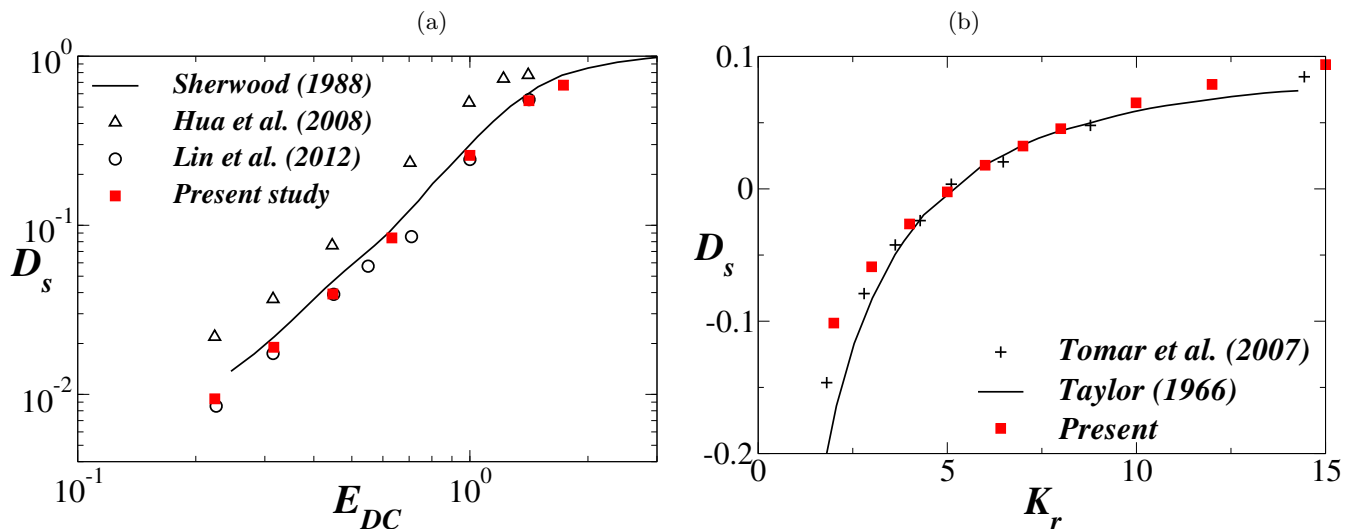


FIG. 3: The variations of D_s with (a) the applied DC electric field, E_{DC} for $Re = 3.64$ and $S = 5$ (perfect dielectric medium), and (b) the electrical conductivity ratio, K_r for $Re = 0.746$, $O_c = 2.68$, $E_{DC} = 0.428$ and $S = 10$ (leaky dielectric medium).

B. Numerical method

A volume-of-fluid (VoF) method based on a finite volume framework is used to simulate the electrohydrodynamics of a droplet in a conducting medium. An open source fluid flow solver, *Basilisk* [18] is used that employs a height-function based balanced force continuum surface force (CSF) formulation for the computation of the surface tension force. A charge-conservative approach is implemented by including the electric force into the Navier-Stokes equations [8] considering both convection and conduction of the free charges. The numerical method used in the present study is similar to that of [8], where several validation exercises were also performed for a leaky dielectric model.

In order to validate our flow solver, in Fig. 3(a) and (b), the deformations of the droplet under the application of a DC electric field in perfect dielectric and leaky dielectric media have been compared against the previous results. In all the cases, the system is assumed to be neutrally buoyant and the simulations are performed till the steady state is reached. It can be seen in Fig. 3(a) that in case of the perfectly dielectric medium for $Re = 3.64$ and $S = 5$, the droplet elongates from its initially spherical shape as the time progresses and eventually reaches to a steady prolate ellipsoid shape. The degree of deformation at the steady state is denoted by D_s . With the increase in the DC electric field strength (E_{DC}), the steady degree of deformation, D_s increases, i.e. the droplet becomes more prolate. We also see that the results obtained from the present simulations agree well with the previous theoretical [21] and computational [6, 7] studies.

In Fig. 3(b), we compare the results obtained from the present solver in case of a leaky dielectric medium with the previous computational [28] and theoretical [26] studies. The parameters considered are $Re = 0.746$, $O_c = 2.68$, $E_{DC} = 0.428$ and $S = 10$. [26] conducted a linearised asymptotic analysis by assuming both the fluids to be conducting and highly viscous (low Re), and derived an expression for D_s , which is given by (in the dimensionless form)

$$D_s = \frac{9}{16} \frac{E_0^2}{(2 + K_r)^2} \left[1 + K_r^2 - 2S + \frac{3}{5}(K_r - S) \frac{2 + 3\mu_r}{1 + \mu_r} \right], \quad (11)$$

where μ_r is the ratio of viscosity of the droplet and the outer fluid, which is set to one in the present study. As in [28], a square computational domain of dimensionless length equals to 20 is considered for this case only. Note that the rest of the results presented in this study are generated using a computational domain of dimensionless length equals to 8. The numerical simulations are performed for different values of K_r . It can be seen in Fig. 3(b) that the droplet exhibits an oblate shape at low values of K_r , and upon increasing the value of K_r the droplet deforms to a prolate shape via a spherical shape at an intermediate value of K_r . Moreover, the present simulations show excellent agreement with the previous studies.

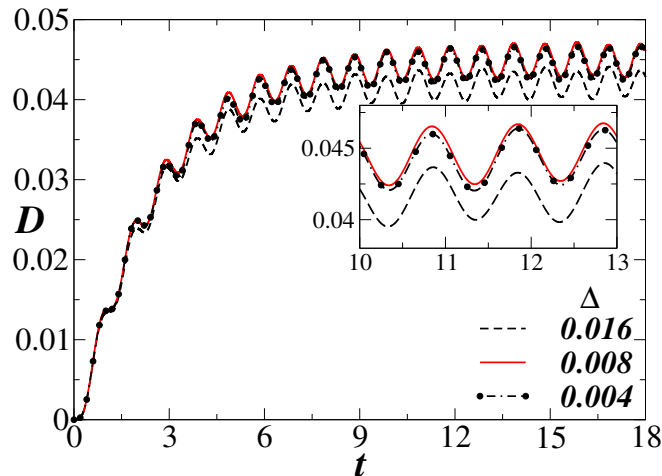


FIG. 4: The temporal variations of D obtained using three different grids under an AC electric field with $E_0 = 0.5$ ($\psi_0 = 4$) and $T_p = 2$. The remaining parameter values are $Re = 1$, $O_c = 10$, $S = 10$ and $K_r = 2$. The inset is a zoomed view showing the oscillations of D at $10 \leq t \leq 13$.

C. Grid convergence test

As the main focus of the present study is to investigate the droplet deformation dynamics under the influence of an AC electric field, in Fig. 4, we have conducted a grid convergence test for a typical set of parameters under the influence of an AC field. The parameters considered for these simulations are $E_0 = 0.5$ (corresponds to $\psi_0 = 4$) and $T_p = 2$ with the remaining parameter values being $Re = 1$, $O_c = 10$, $S = 10$ and $K_r = 2$. The simulations are performed using three meshes with cell sizes, $\Delta = 0.016$, 0.008 and 0.004 . It can be seen that degree of deformation, D undergoes an oscillatory variation in this case. Inspection of Fig. 4 reveals that we get acceptable grid-converged results for $\Delta \leq 0.008$, but the result obtained using $\Delta = 0.016$ under-predicts the degree of deformation of the droplet. Thus, $\Delta = 0.008$ is used to generate the rest of the results presented in this study.

III. RESULTS AND DISCUSSION

We begin the presentation of our results by highlighting that the three-dimensional or the axisymmetric simulations are qualitatively different from the two-dimensional ones as conducted by several researchers previously (see for instance, [3, 5, 34]). [29] derived an expression for the degree of deformation, D for a droplet in an unbounded axisymmetric domain in the creeping flow regime under the influence of an AC electric field ($E_{AC}(t) = E_0 \cos(2\pi t/T_p)$). They reported that D can be expressed as a sum of mean (D_m) and oscillatory (D_o) parts, i.e. $D = D_m + D_o$. The mean deformation (D_m) is found to be the same as the steady state deformation (D_s) in case of a DC electric field with $E_{DC} = E_{rms,AC} = E_0/\sqrt{2}$ (see Eq. (2)) under the condition that $S = K_r$ (i.e. along the zero circulation line as shown in Fig. 1). However, by performing two-dimensional simulations, [5] observed similar mean behaviour for the deformation of the droplet under the influence of AC and DC electric fields even for the points away from the zero circulation line. Hereafter, the mean deformation (D_m) in the AC field and the steady state deformation in the DC field are represented by one symbol, D_s .

In Fig. 5(a), the comparison of temporal variations of D obtained from our two-dimensional simulations for a point slightly away from the $S = K_r$ line ($S = 10$ and $K_r = 6$; point 1 located in region II of Fig. 1) shows a good match between the mean behaviour of the AC and DC electric fields. In order to check whether this is true in case of a more realistic, axisymmetric simulation, the corresponding results for the AC and the equivalent DC cases are presented in Fig. 5(b). It can be seen that the degree of deformations for the AC and DC cases differ significantly. This motivates us to consider a point on the $S = K_r$ line, and the results for such a point ($S = 10$ and $K_r = 10$; point 2 located in the $S = K_r$ line of Fig. 1) are shown in Fig. 5(c), which shows a very good agreement between the AC and DC cases. Further, we investigated the variation of D for different values of T_p in case of a AC field with $S = 10$ and $K_r = 10$ and observed (not shown) that the mean behaviour to be the same under the influence of AC and DC electric fields. It is to be noted here that although the theory developed by [29] corresponds to the creeping flow regime, it predicts the behaviour well even for $\mathcal{O}(1)$ Reynolds numbers.

Next, in Fig. 6(a), we study effect of the time period (T_p) of the applied AC field with $\psi_0 = 4$ on the deformation of

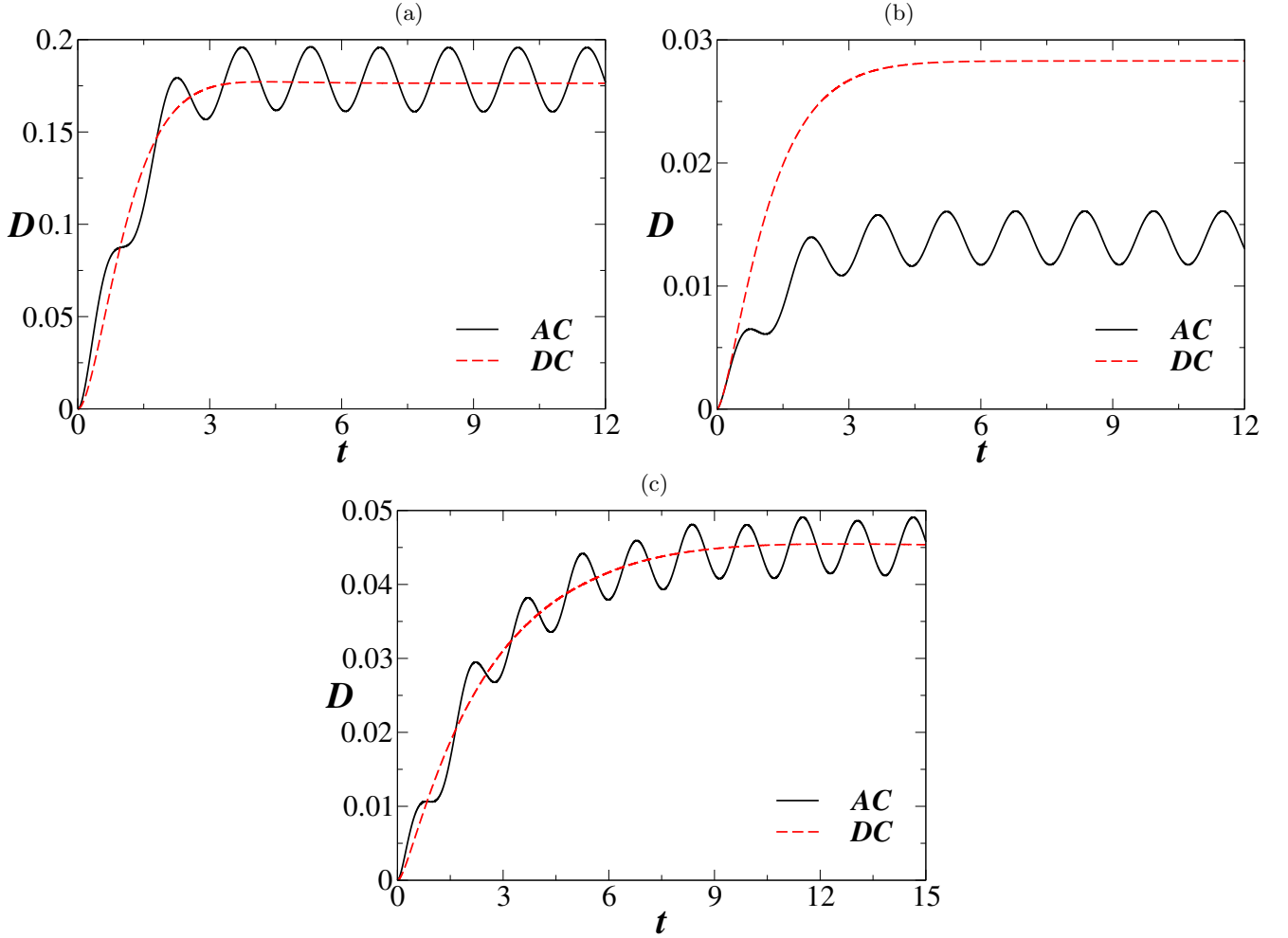


FIG. 5: The temporal variations of D . (a) two-dimensional and (b) axisymmetric simulations for $S = 10$ and $K_r = 6$; the values of potential in the AC and DC electric fields are $\psi_0 = 2.5$ and $\psi_{DC} = 2.5/\sqrt{2}$, respectively. (c) Axisymmetric simulations for $S = 10$ and $K_r = 10$; the values of potential in the AC and DC electric fields are $\psi_0 = 4$ and $\psi_{DC} = 4/\sqrt{2}$, respectively. $T_p = \pi$ is considered for all the AC cases. The remaining parameter values are $Re = 2$, $O_c = 0.01$, $S = 10$ and $K_r = 6$.

the droplet at point 3 ($S = 10$ and $K_r = 2$) in Fig. 1. Note that point 3 in Fig. 1 lies in region I; away from the zero circulation ($S = K_r$) line. The remaining parameter values are $Re = 1$ and $O_c = 10$. It can be seen that an initially spherical droplet undergoes periodic shape oscillations under the application of AC electric field. Increasing the value of T_p increases the amplitude and time period of oscillations of the droplet. We observe that for low values of T_p , the droplet deforms to a prolate shape ($D > 0$) and undergoes shape oscillations about a mean degree of deformation, D_s (see $T_p \leq 10$ in Fig. 6(a)). For a high value of T_p (see for instance, $T_p = 50$ in Fig. 6(a)), the droplet undergoes periodic oscillations, but during the oscillations it deforms between a slight oblate shape to a large prolate shape. The shape oscillations of the droplet becomes complex for high values of T_p (see $T_p \geq 10$). Close inspection of Fig. 6(a) also reveals that the time period of shape oscillations of the droplet is about $T_p/2$ as also observed in earlier studies (e.g. [5]).

In Fig. 6(b), we investigate whether there exists an equivalent DC electric field, E_{DC} whose steady degree of deformation will be the same as the mean degree of deformation of the AC electric field. The electric potential of the DC field (ψ_{DC}) is varied, such that ψ_{DC} equals to $\psi_0/2\sqrt{2}$, $\psi_0/\sqrt{2}$, ψ_0 and $\sqrt{2}\psi_0$. It can be seen that for all the values of ψ_{DC} , keeping the rest of the parameters the same as Fig. 6(a), the degree of deformation of the droplet increases to a maximum value (prolate shape) and subsequently decreases to reach to a steady oblate shape. Increasing the value of ψ_{DC} increases the maximum value of D . As shown by [29], this result also proves that there is no similarity between the dynamics of a droplet under AC and DC electric fields for $S \neq K_r$.

In order to understand the dynamics of the droplet under the action of AC ($T_p = 2$) and DC ($\psi_{DC} = \psi_0/\sqrt{2}$) electric fields, we present the pressure field with the velocity vectors at different times in Fig. 7(a) and (b), respectively. The

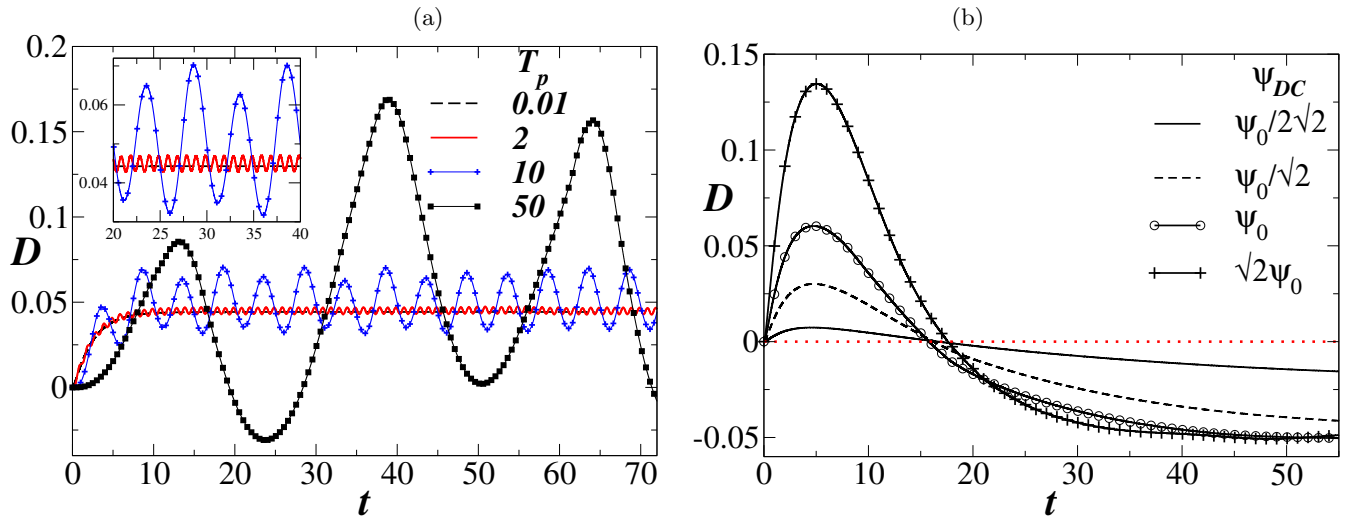


FIG. 6: The temporal variations of D under the influence of an (a) AC electric field for $\psi_0 = 4$ with different values of T_p , and (b) DC electric field for different values of ψ_{DC} . The remaining parameter values are $Re = 1$, $O_c = 10$, $S = 10$ and $K_r = 2$. The inset in panel (a) presents the zoomed view.

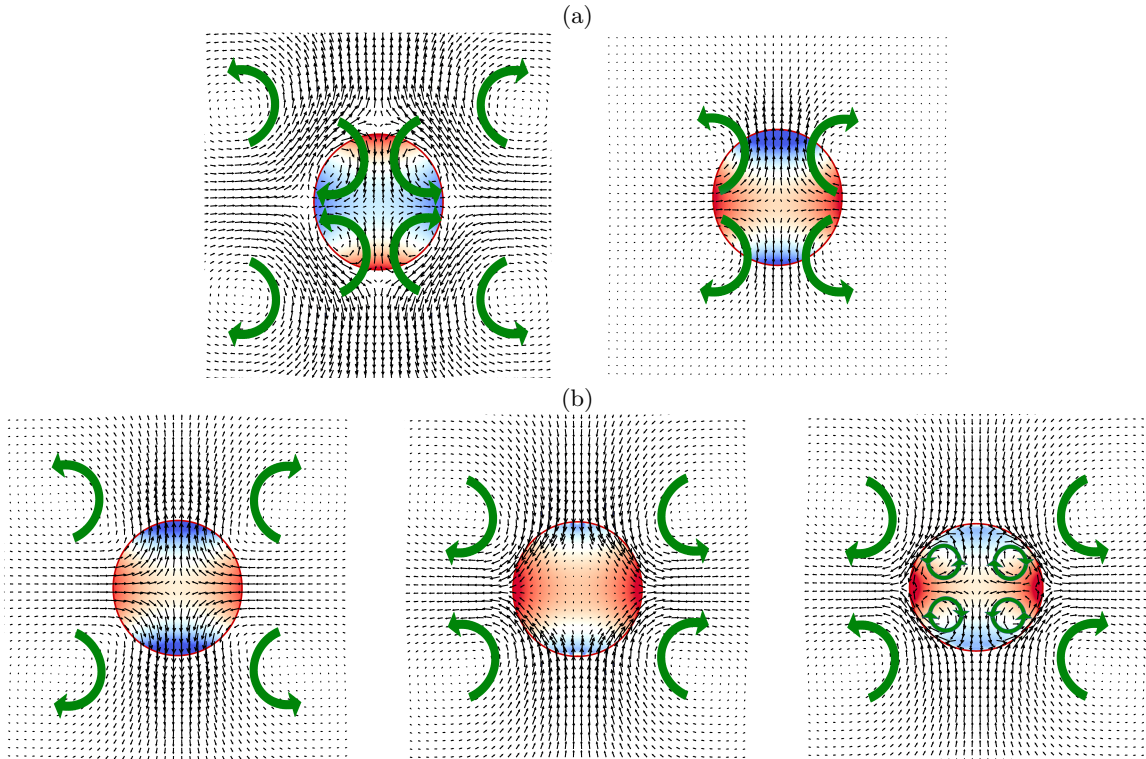


FIG. 7: The pressure field with the velocity vectors at different times. (a) AC electric field with $T_p = 2$: $t = 2$ (left panel) and $t = 2.5$ (right panel) and (b) DC electric field with $\psi_{DC} = \psi_0/\sqrt{2}$: at $t = 2$ (left panel), $t = 10$ (middle panel) and $t = 30$ (right panel). The remaining parameter values are the same as Fig. 6.

remaining parameter values are the same as Fig. 6. In Fig. 7(a), $t = 2$ and $t = 2.5$ correspond to one peak and the next trough of the oscillations observed in the AC field with $T_p = 2$. It can be seen that at $t = 2$ (when the droplet reaches to a prolate shape), the pressure is high at poles and low at the equator of the droplet which results in a flow from the high pressure region to the low pressure region. This in turn creates recirculation of opposite sign in the outer fluid. At $t = 2.5$, the pressure is low at the poles as the droplet deforms to an oblate shape, and thereby constituting a flow from the equator to poles of the droplet. This behaviour is found to be similar for other values of

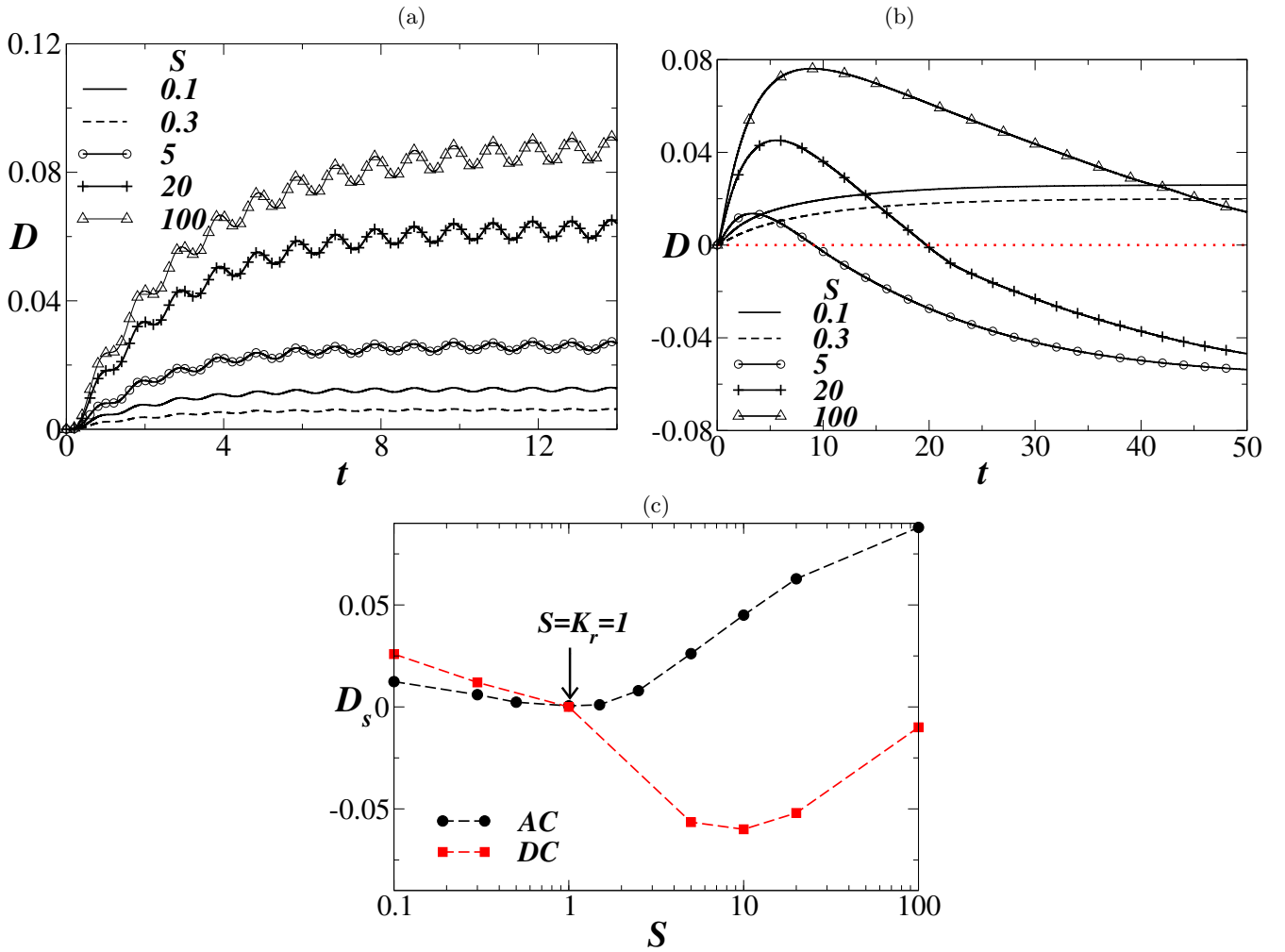


FIG. 8: The temporal variations of D for different values of S for $K_r = 1$. (a) AC electric field ($E_0 = 0.5$, $T_p = 2$) and (b) DC electric field ($E_{DC} = E_0/\sqrt{2}$). (c) The variation of steady mean degree of deformation, D_s of the droplet with S for the AC and DC electric fields. The remaining parameter values are $Re = 1$ and $O_c = 10$.

T_p .

In case of the DC electric field with $\psi_{DC} = \psi_0/\sqrt{2}$, we plot the pressure field and velocity vectors at $t = 2, 10$ and 30 in Fig. 7(b). It can be seen that at $t = 2$ (when the droplet is deforming towards its maximum prolate shape), the pressure is high in the equatorial plane of the droplet, which increases with time (see at $t = 10$). This creates a strong recirculating flow in the outer fluid. When the droplet deforms towards its final steady state ($t = 30$), four symmetrically closed recirculating regions appear inside the droplet.

Then, we perform a parametric study by varying the permittivity ratio, S for $K_r = 1$ and the electrical conductivity ratio, K_r for $S = 10$. The remaining parameters are $Re = 1$ and $O_c = 10$. In Fig. 8(a) and (b), the temporal variations of D for different values of S for the AC electric field with $E_0 = 0.5$ and $T_p = 2$, and the equivalent DC electric field with $E_{DC} = E_0/\sqrt{2}$ are presented, respectively. Nine values of S are considered which are associated with points 4 ($S = 0.1$), 5 ($S = 0.3$), 6 ($S = 5$), 7 ($S = 20$), 8 ($S = 100$), 10 ($S = 10$), 14 ($S = 0.5$), 15 ($S = 1.5$) and 16 ($S = 2.5$) in Fig. 1. It can be seen in Fig. 8(a) that under the action of AC electric field, the droplet becomes prolate (elongates in the direction of electric field) and oscillates about a mean value of D for all values of S considered. For $S = 0.1$ and 0.3 , the droplet slightly deforms and reaches to a prolate shape (with mean degree of deformation, D_s) with small amplitude shape oscillations. The steady mean degree of deformation, D_s of the droplet shows a non-monotonic trend with a minimum value for $S = 1$ for this set of parameters. Increasing the permittivity ratio further (i.e. $S \geq 1$) increases the value of D_s (see Fig. 8(c)). The amplitude of oscillations about the mean value of D also increases with increasing S . However, the time period of oscillations is constant for all values of S , which is found to be half of the time period of the applied electric field, T_p .

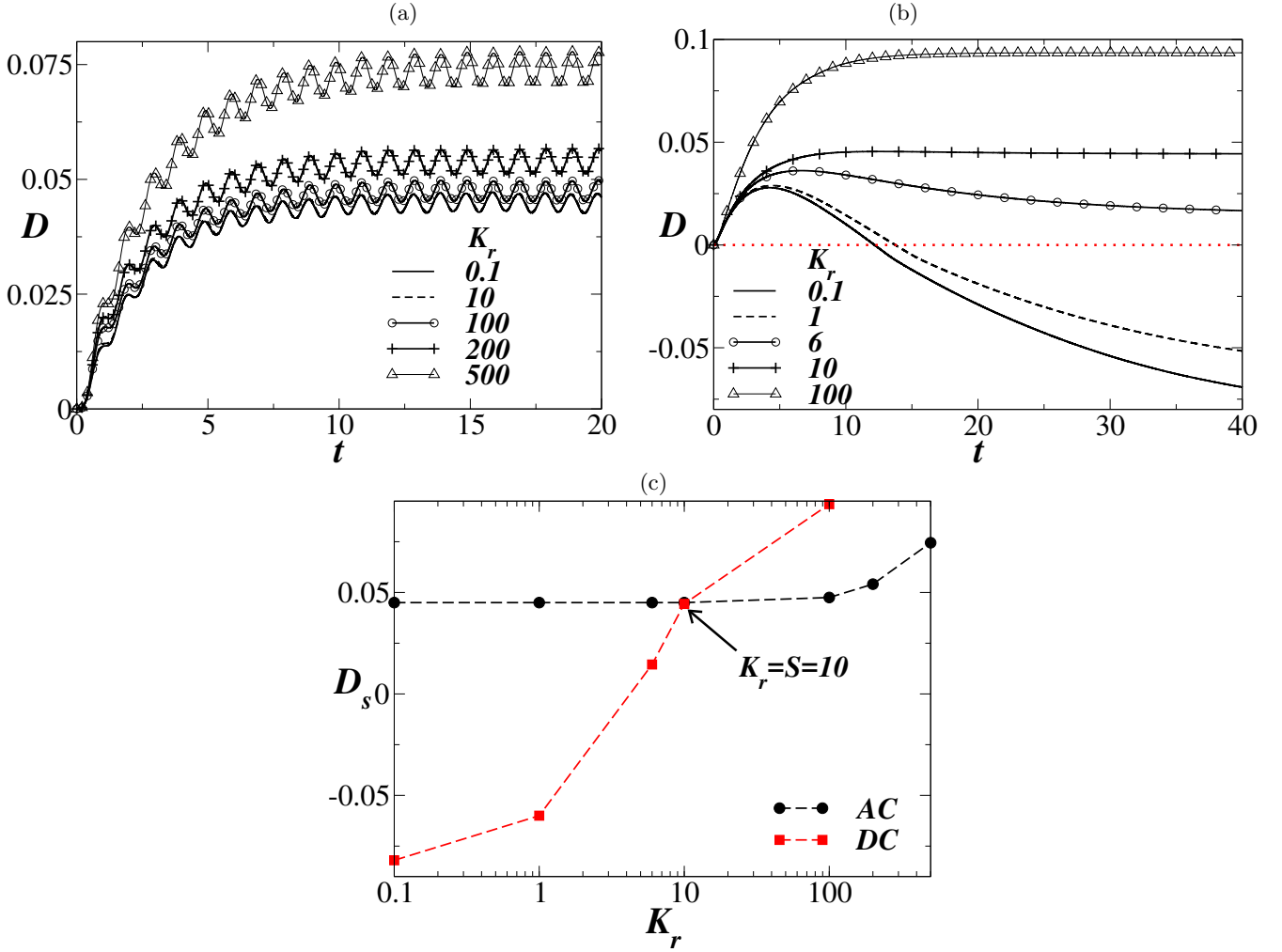


FIG. 9: The temporal variations of D for different values of K_r for $S = 10$. (a) AC electric field ($E_0 = 0.5$, $T_p = 2$) and (b) DC electric field ($E_{DC} = E_0/\sqrt{2}$). (c) The variation of steady mean degree of deformation, D_s of the droplet with K_r for the AC and DC electric fields. The remaining parameter values are $Re = 1$ and $O_c = 10$.

The dynamics of the droplet under the application of the equivalent DC electric field with $E_{DC} = E_0/\sqrt{2}$ is very different from that observed in the AC field as shown in Fig. 8(b). In this case, for low values of S (see the results for $S = 0.1$ and 0.3 , at points 4 and 5 in Fig. 1), the droplet deforms to a steady prolate shape; however, the value of D_s decreases with increasing the value of S . Note that points 4 and 5 lies in region III. For points in region I, i.e. for $S = 5, 20$ and 100 in Fig. 8(b), it can be seen that the droplet initially deforms to a prolate shape (elongation) reaches to a maximum value, followed by a contraction in the direction of electric field and eventually reaches to a steady oblate shape (see Fig. 8(c)). The time taken by the droplet to reach to its maximum prolate and the final steady state increases with increasing the value of S .

The temporal variations of D for $K_r = 0.1$ (point 9), 10 (point 2), 100 (point 11), 200 (point 12) and 500 (point 13) under the action of the AC electric field with $E_0 = 0.5$ and $T_p = 2$ are presented in Fig. 9(a). For the range of K_r values considered, the droplet deforms to a prolate shape and exhibits a periodic oscillations with time period half of that of the applied electric field. It can be observed that below the $S = K_r$ (the zero-circulation line) in Fig. 1, increasing K_r has a negligible effect on the deformation dynamics of the droplet for the set of parameters considered in the present study. Above $S = K_r$ line, increasing K_r increases the steady/mean degree of deformation of the droplet, D_s (see Fig. 9(c)). The amplitude of oscillations about the mean value of D ; however with a constant time period, is found to be increased with the increase in the value of K_r . On the other hand, under the action of an equivalent DC electric field ($E_{DC} = E_0/\sqrt{2}$), it can be seen in Fig. 9(b) that in region I of Fig. 1, the droplet deforms to a steady oblate shape after deforming to an early prolate shape (see the results for $K_r = 0.1$ (point 9) and $K_r = 1$ (point 10)). Above the zero-deformation curve, the droplet deforms as the time progresses and reaches a steady prolate shape (see

the results of $K_r = 6$ (point 1), $K_r = 10$ (point 2) and $K_r = 100$ (point 11)). Close inspection of Fig. 9(b) also reveals that for $K_r < S$, the droplet always reaches to an intermediate prolate shape, followed by a decrease in the degree of deformation, and finally the droplet obtains its final steady shape. The time scale for the charge relaxation from the outer fluid to the interface is given by $\tau = \epsilon/K$. Thus, the ratio of charge relaxation times of the inner fluid to outer fluid is S/K_r . For $S > K_r$, the free charges in the inner fluid take longer time to relax to the interface as compared to the free charges in the outer fluid. This causes an initial motion of the charges towards the pole of the droplet, thus the droplet becomes prolate, initially. Subsequently, as the charges relax in the inner fluid, the steady state charge distribution governs the final shape of the droplet. It can be observed in Figs. 8(c) and 9(c) that the values of D_s are same in the AC and DC electric fields when $K_r = S$, as observed by [29]. They also experimentally observed that for high permittivity and low electrical conductivity ratios, the droplet eventually obtains a prolate shape and an oblate shape under the application of AC and equivalent DC electric fields, respectively.

IV. CONCLUDING REMARKS

The electrohydrodynamics of an initially spherical droplet in a leaky dielectric medium under the influence of an external AC electric field is investigated via axisymmetric numerical simulations. In order to isolate the effect of electric field, the system is considered to be neutrally buoyant and the dynamic viscosity of the droplet and the surrounding medium are assumed to be the same. A charge-conservative volume-of-fluid (VoF) based finite volume flow solver, *Basilisk* [18] is used. The implementation of the electrohydrodynamics in the present study is similar to that of [8]. The present solver has been extensively validated against the previous theoretical [26] and computational studies for both perfect [6, 7, 21] and leaky dielectric media [28]. A grid convergence test is also conducted to obtain an optimal grid to be used in the present study. We compare the results obtained under the action of an AC electric field with the corresponding results of an equivalent DC electric field.

The present study is motivated from the fact that there is discrepancy between the experimental results of [29] and the previous two-dimensional simulations. [29] reported that along the zero circulation line (i.e. $S = K_r$ line), the mean deformation of a droplet in an AC electric field is the same as the steady state deformation in a DC electric field with a field strength equal to the root-mean-square value of the AC electric field strength. However, in two-dimensional simulations, it is observed that the mean behaviours for the droplet deformation under the influence of AC and DC electric fields are same even for the points away from the zero circulation line ($S = K_r$) shown in Fig. 1.

The main contributions from the present study are in three-fold. (i) The droplet deformation dynamics in case of an AC electric field is found to be strikingly different from that observed in case of an equivalent DC field for $K_r \neq S$. (ii) The results obtained from our axisymmetric simulations are consistent with the experimental investigation of [29], thereby indicating that two-dimensional simulations do not predict the actual behaviour of the droplet deformation. (iii) A parametric study is conducted by varying the time period of the applied AC electric field, T_p , the permittivity ratio, S and the electrical conductivity ratio, K_r . Sixteen pairs of K_r and S values are considered. The droplet deformation and the flow field associated with the AC electric field for each pair of K_r and S are compared with those obtained with the equivalent DC electric field. Our study reveals that in case of an AC electric field, the droplet oscillates about a prolate shape, whose amplitude of oscillations increases with the increase in the value of T_p . However, the time period of these oscillations is always observed to be equal to $T_p/2$; i.e. the dynamics in this case is subharmonic. Increasing the value of S and K_r has a nonmonotonic effect on the degree of deformation of the droplet exhibiting a minimum at $K_r = S$. In contrast to the dynamics observed in an AC field, in case of the equivalent DC electric field, for $K_r < S$, the droplet deforms to a steady oblate shape after deforming to an early prolate shape, but for $K_r > S$, the droplet continues to deforms monotonically and obtains a steady prolate shape.

Acknowledgement: K. C. S. thanks DST - MATRICS India for the financial support through the grant MTR/2017/000029.

-
- [1] BANDOPADHYAY, A., MANDAL, S., KISHORE, N. K. & CHAKRABORTY, S. 2016 Uniform electric-field-induced lateral migration of a sedimenting drop. *J. Fluid Mech.* **792**, 553–589.
 - [2] BASARAN, O. A., GAO, H. & BHAT, P. P. 2013 Nonstandard inkjets. *Ann. Rev. Fluid Mech.* **45**, 85–113.
 - [3] BEHJATIAN, A. & ESMAEELI, A. 2013 Electrohydrodynamics of a liquid column under a transverse electric field in confined domains. *Int. J. Multiphase Flow* **48**, 71–81.
 - [4] DAS, D. & SAINTILLAN, D. 2017 Electrohydrodynamics of viscous drops in strong electric fields: numerical simulations. *J. Fluid Mech.* **829**, 127–152.

- [5] ESMAEELI, A. & HALIM, MD. A. 2018 Electrohydrodynamics of a liquid drop in ac electric fields. *Acta Mech.* **229** (9), 3943–3962.
- [6] HUA, J., LIM, L. K. & WANG, C-H 2008 Numerical simulation of deformation/motion of a drop suspended in viscous liquids under influence of steady electric fields. *Phys. Fluids* **20** (11), 113302.
- [7] LIN, Y., SKJETNE, P. & CARLSON, A. 2012 A phase field model for multiphase electro-hydrodynamic flow. *Int. J. Multiphase Flow* **45**, 1–11.
- [8] LÓPEZ-HERRERA, J. M., POPINET, S. & HERRADA, M. A. 2011 A charge-conservative approach for simulating electrohydrodynamic two-phase flows using volume-of-fluid. *J. Comput. Phys.* **230** (5), 1939–1955.
- [9] MANDAL, S., BANDOPADHYAY, A. & CHAKRABORTY, S. 2016 Effect of surface charge convection and shape deformation on the dielectrophoretic motion of a liquid drop. *Phys. Rev. E.* **93** (4), 043127.
- [10] MANDAL, S., BANDOPADHYAY, A. & CHAKRABORTY, S. 2017 The effect of surface charge convection and shape deformation on the settling velocity of drops in nonuniform electric field. *Phys. Fluids* **29** (1), 012101.
- [11] MANDAL, S., CHAKRABARTI, S. & CHAKRABORTY, S. 2017 Effect of nonuniform electric field on the electrohydrodynamic motion of a drop in poiseuille flow. *Phys. Fluids* **29** (5), 052006.
- [12] MANDAL, S. & CHAKRABORTY, S. 2017 Influence of interfacial viscosity on the dielectrophoresis of drops. *Phys. Fluids* **29** (5), 052002.
- [13] MELCHER, J. R. & TAYLOR, G. I. 1969 Electrohydrodynamics: a review of the role of interfacial shear stresses. *Ann. Rev. Fluid Mech.* **1** (1), 111–146.
- [14] MOCHIZUKI, T. 2013 Periodic deformation of microsize droplets in a microchannel induced by a transverse alternating electric field. *Langmuir* **29** (41), 12879–12890.
- [15] NATH, B., BISWAS, G., DALAL, A. & SAHU, K. C. 2018 Cross-stream migration of drops suspended in poiseuille flow in the presence of an electric field. *Phys. Rev. E.* **97** (6), 063106.
- [16] O’KONSKI, C. T. & THACHER JR, H. C. 1953 The distortion of aerosol droplets by an electric field. *J. Phys. Chem.* **57** (9), 955–958.
- [17] PODDAR, A., MANDAL, S., BANDOPADHYAY, A. & CHAKRABORTY, S. 2018 Sedimentation of a surfactant-laden drop under the influence of an electric field. *J. Fluid Mech.* **849**, 277–311.
- [18] POPINET, S. 2009 An accurate adaptive solver for surface-tension-driven interfacial flows. *J. Comput. Phys.* **228**, 5838–5866.
- [19] SANTRA, S., MANDAL, S. & CHAKRABORTY, S. 2018 Electrohydrodynamics of confined two-dimensional liquid droplets in uniform electric field. *Phys. Fluids* **30** (6), 062003.
- [20] SAVILLE, D. A. 1997 Electrohydrodynamics: the taylor-melcher leaky dielectric model. *Ann. Rev. Fluid Mech.* **29** (1), 27–64.
- [21] SHERWOOD, J. D. 1988 Breakup of fluid droplets in electric and magnetic fields. *J. Fluid Mech.* **188**, 133–146.
- [22] SIMPSON, G. C. & WALKER, G. T. 1909 On the electricity of rain and its origin in thunderstorms. *Phil. Trans. R. Soc. Lond. A* **209**, 379–413.
- [23] SINGH, R., BAHGA, S. S. & GUPTA, A. 2018 Electrohydrodynamics in leaky dielectric fluids using lattice boltzmann method. *Eur. J. Mech. B-Fluid.* **74**, 167–179.
- [24] STONE, H. A., STROOCK, A. D. & AJDARI, A. 2004 Engineering flows in small devices: microfluidics toward a lab-on-a-chip. *Ann. Rev. Fluid Mech.* **36**, 381–411.
- [25] TAYLOR, G. I. 1966 Studies in electrohydrodynamics. i. the circulation produced in a drop by an electric field. *Proc. R. Soc. Lond. A* **291** (1425), 159–166.
- [26] TAYLOR, G. I. 1966 Studies in electrohydrodynamics, i: The circulation produced in a drop by electrical field. *Proc. R. Soc. London, Ser. A.* **291**, 159–166.
- [27] THAKAR, R. M. 2012 Dielectrophoresis and deformation of a liquid drop in a non-uniform, axisymmetric ac electric field. *Eur. Phy. J. E.* **35** (8), 76.
- [28] TOMAR, G., DANIEL, G., BISWAS, G., NORBERT, A., SHARMA, A., DURST, F., WELCH, S. W. J. W. & DELGADO, A. 2007 Two-phase electrohydrodynamic simulations using a volume-of-fluid approach. *J. Comput. Phys.* **227** (2), 1267–1285.
- [29] TORZA, S., COX, R. G. & MASON, S. G. 1971 Electrohydrodynamic deformation and bursts of liquid drops. *Phil. Trans. R. Soc. Lond. A* **269** (1198), 295–319.
- [30] VIZIKA, O. & SAVILLE, D. A. 1992 The electrohydrodynamic deformation of drops suspended in liquids in steady and oscillatory electric fields. *J. Fluid Mech.* **239**, 1–21.
- [31] VLAHOVSKA, P. M. 2019 Electrohydrodynamics of drops and vesicles. *Ann. Rev. Fluid Mech.* **51**, 305–330.
- [32] WANG, Y., SUN, D., ZHANG, A. & YU, B. 2017 Numerical simulation of bubble dynamics in the gravitational and uniform electric fields. *Numer. Heat Tr. A-Appl.* **71** (10), 1034–1051.
- [33] WHYBREW, W. E., KINZER, G. D. & GUNN, R. 1952 Electrification of small air bubbles in water. *J. Geophys. Res.* **57** (4), 459–471.
- [34] YANG, Q., LI, B. Q. & XU, F. 2017 Electrohydrodynamic rayleigh-taylor instability in leaky dielectric fluids. *International Journal of Heat and Mass Transfer* **109**, 690–704.
- [35] ZABARANKIN, M. 2017 Liquid toroidal drop under uniform electric field. *Proc. R. Soc. A* **473** (2202), 20160633.